

# Geomechanical risk assessment for CO<sub>2</sub> storage in the North Sea's Luna site: A seismic-driven coupled compositional flow and geomechanics approach

Amir Haghi\*, Philippa Park, and Robert Porjesz, Viridien

## Summary

A comprehensive assessment of geomechanical risks is essential for the success of geological carbon storage. Although the relationship between injection-induced pore pressure changes and rock failure is broadly understood in poromechanics, the challenge of characterizing and managing geomechanical hazards associated with subsurface CO<sub>2</sub> injection in saline aquifers persists, affecting its viability as a global strategy for achieving a net-zero carbon economy. Here, we investigate the geomechanical response of the Luna saline aquifer in the North Sea to CO<sub>2</sub> injection using coupled compositional flow and geomechanics simulations based on a seismic-driven high-fidelity static model. We find a surface uplift of 13 mm following a constant injection rate of  $1.5 \times 10^6$  m<sup>3</sup>/d (i.e., 1 Mt/y) in the Luna aquifer for 20 years, which is considered reasonable and safe for offshore surface facilities. We show that the upper limits of shear stress level (SSL) and tensile stress level (TSL) are 0.5 and 0.78, respectively, in both the reservoir and caprock. Since SSL and TSL values below 0.8 are considered safe, our results suggest that gas injection-induced reservoir and caprock failure is unlikely in the study area, providing confidence that caprock mechanical leakage poses a low risk for long-term CO<sub>2</sub> storage.

## Introduction

Geological storage of carbon dioxide is a crucial component of the transition to a net-zero carbon economy (IEA, 2021). Comprehensive geomechanical modeling of subsurface CO<sub>2</sub> injection in saline aquifers is essential for investigating CO<sub>2</sub> plume migration (Bachu and Adams, 2003), pressure buildup (Zhao et al., 2012), and potential risks, including surface uplift (Rutqvist, 2012), wellbore and caprock integrity issues (Han et al., 2024), and induced seismicity (Hager et al., 2021). Much of the research on CO<sub>2</sub> injection modeling in saline aquifers has adopted reservoir-scale models focused on the shape and distribution of the CO<sub>2</sub> plume (Wang et al., 2023). Compositional fluid flow simulation allows for the dissolution of CO<sub>2</sub> in brine, which is essential for accurate plume modeling (Pruess and García, 2002). Far less emphasis has been placed on the scale and resolution of the static model (both reservoir and overburden), pressure plume distribution, and the associated geomechanical risks within and around the reservoir. Despite recent advances in geomechanical simulation, coupled compositional fluid flow and geomechanical modeling based on high-resolution 3D seismic imaging remains a significant challenge, particularly for CO<sub>2</sub> injection in offshore saline aquifers.

CO<sub>2</sub> injection into a saline aquifer causes pore pressure buildup in the brine-saturated porous formation, with the magnitude of pressure increases depending on the distance from the injector (Zeidouni, 2024). According to poroelasticity theory, this leads to an increase in total stress, a decrease in effective stress, and rock deformation (Terzaghi, 1943; Biot, 1941; Haghi and Chalaturnyk, 2024; Haghi et al., 2019, 2020, 2021). Excessive deformation can induce inelastic deformation and rock failure, either through shear failure or tensile fracturing. Shear failure occurs when the shear stress ( $\tau$ ) exceeds the shear strength of the rock, which follows the Mohr-Coulomb failure criterion:  $\tau = C_0 + \mu\sigma_n$ , where  $C_0$  is the cohesion,  $\mu$  is the friction coefficient, and  $\sigma_n$  is the normal effective stress at failure. According to frictional equilibrium theory, in the faulted Earth's crust, a zero cohesion assumption ( $C_0 = 0$ ) and a friction coefficient of  $\mu = 0.6$  are commonly recommended (Zoback, 2011; Haghi et al., 2013, 2018). Tensile failure occurs when the pore pressure ( $P_p$ ) exceeds the minimum principal stress ( $S_3$ ), leading to abrupt fracturing, typically perpendicular to the maximum stress direction or along subsurface interfaces such as bedding planes, faults, or pre-existing fractures (Sibson, 2017; Yang et al., 2025). In contrast to the wealth of numerical simulations focusing on CO<sub>2</sub> plume migration in saline aquifers, the modeling of pore pressure plumes and their destructive geomechanical impact remains relatively underexplored. This is despite global observations demonstrating the significant effects of pressure perturbations on fault reactivation and caprock failure, which can propagate far from the injection site (Zoback and Gorelick, 2012; Rutqvist, 2008). Accurate CO<sub>2</sub> pressure plume modeling and geomechanical risk assessment require large-scale models that encompass the reservoir, overburden, underburden, and sideburden (Vilarrasa and Carrera, 2015). Additionally, high-resolution, seismic-driven static models are essential to capture the structural details along subsurface interfaces necessary for geomechanical modeling (Sengupta et al., 2011). However, a robust modeling approach that fully integrates compositional fluid flow—between gaseous and aqueous phases—and mechanical deformation within a high-resolution, seismic-driven static model remains largely unexplored.

Here, we use a seismic-driven, coupled numerical approach to study the geomechanical risks of CO<sub>2</sub> sequestration in the Luna saline aquifer in the North Sea, focusing on assessing the potential for reservoir or caprock failure and identifying key factors that control these risks. To address this challenge, we develop a high-fidelity static model with 15.5 million grid cells, incorporating reservoir, overburden, and

## Geomechanical risk assessment for CO<sub>2</sub> storage in the North Sea's Luna site

underburden properties derived from 3D seismic inversion and well-log data. We then perform coupled compositional flow and geomechanics simulations to investigate CO<sub>2</sub> plume migration, pressure distribution, surface uplift, and failure analysis using the Coulomb failure criterion. Our results reveal the significant influence of stress anisotropy, structural heterogeneity, and rock properties on the asymmetric CO<sub>2</sub> plume shape and pressure distribution after 20 years of injection. This study highlights the importance of adapting a robust simulation workflow for geomechanical risk mitigation in CO<sub>2</sub> sequestration operations within the Luna aquifer, which can be extended to CO<sub>2</sub> storage projects in the North Sea or similar geological settings.

### Luna Storage Site

The Luna site is a potential carbon capture and storage (CCS) initiative in the Norwegian North Sea, located west of the Northern Lights CCS project, at a water depth of approximately 200 meters. The geological structure of the North Sea has been shaped by Upper Jurassic to Lower Cretaceous rifting events, influenced by older tectonic formations. These main rifting events had a significant impact on the present-day structural setting and the quality of pre-rift sandstone reservoirs, including the Statfjord Formation (Norwegian Petroleum Directorate, 2025).

The Luna site aims to store CO<sub>2</sub> in the Statfjord Formation, a Lower Jurassic sandstone reservoir, located at depths between 2500 and 3500 meters beneath the seabed. With high porosity (above 20%) and permeability, the Statfjord Formation is well-suited for CO<sub>2</sub> injection and long-term containment. Overlying Jurassic shale formations, including the Drake Formation, serve as primary caprocks, preventing the upward migration of stored CO<sub>2</sub> (Bretan et al., 2011). Previous studies also indicate the presence of secondary caprock formations (Booth et al., 2021).

### Methodology

#### Static model

We developed a high-fidelity static model with grid dimensions of 1710 × 244 × 37 (15.5 million cells), incorporating the reservoir as well as high-resolution overburden and underburden properties derived from 3D seismic inversion and well-log data (**Error! Reference source not found.**). The model spans an area of 20 × 40 km, with the brine-saturated aquifer located at depths ranging from 2500 m to 3500 m, deepening toward the northeast.

We establish a strong correlation between porosity and acoustic impedance using public well data. We then perform seismic acoustic inversion from below the reservoir up to the seafloor and convert to depth using well data and seismic imaging velocities. Porosity is calculated from impedance values, while permeability is modeled using a well-data-driven porosity-permeability equation.

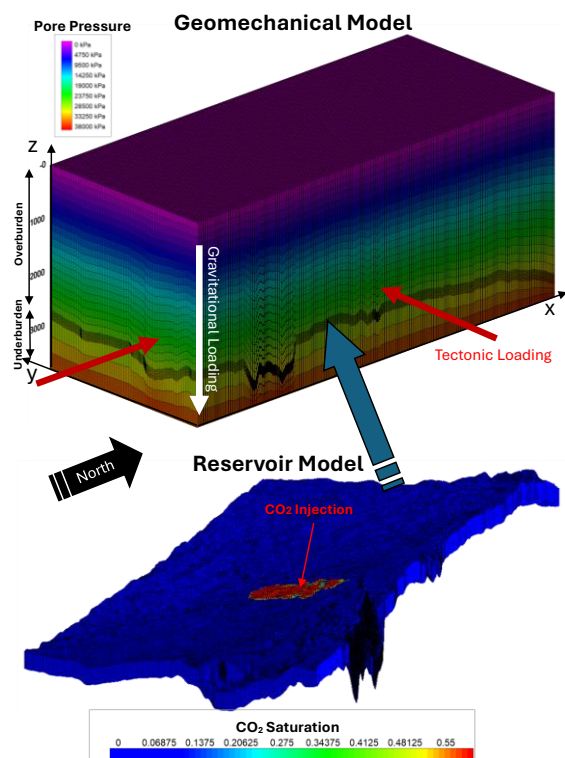


Figure 1: High-resolution reservoir geomechanical model.

#### Compositional reservoir model

We use CMG for compositional reservoir simulation. The model's initial conditions include hydrostatic pore pressure and a temperature of 100°C. A two-component model is established based on the Peng-Robinson equation of state. CO<sub>2</sub> dissolution in brine is modeled using Henry's Law and Harvey's correlation for CO<sub>2</sub> (Harvey, 1996). For relative permeability curves, we adopt Brooks-Corey exponents for mid-range permeability (10–100 mD), along with endpoints and hysteresis effects from published CO<sub>2</sub>-brine core-flooding databases (Bachu, 2013; Burnside & Naylor, 2014). A CO<sub>2</sub> injector is located down-dip into the Statfjord formation with a target injection rate of  $1.5 \times 10^6$  m<sup>3</sup>/d, aiming to inject 1 million tons of CO<sub>2</sub> annually into the aquifer over a 20-year period, starting on January 1, 2065 (**Error! Reference source not found.**).

#### Coupled geomechanical simulation

We use Geosim to perform coupled geomechanical simulations with advanced parallelization capabilities, optimized for high-performance computing (HPC) systems. Using the finite element code within the Geosim simulator, we first initialize the stress field across the entire model through gravitational and tectonic loading, incorporating

## Geomechanical risk assessment for CO<sub>2</sub> storage in the North Sea's Luna site

density, elastic properties, and boundary displacements. During the stress initialization process, we iteratively calibrate the model using in-situ stress data from wells. The resulting 3D Mechanical Earth Model (3D MEM) imports pressure and saturation arrays from the compositional reservoir simulation at each timestep (**Error! Reference source not found.**). The coupled reservoir-geomechanical approach calculates deformation and stress throughout the entire injection scenario.

To provide quantitative insights into the risk of failure, we use two key dimensionless parameters for each cell at each timestep (Haghi et al., 2024): (1) Shear Stress Level (SSL), defined as the ratio of deviatoric stress at current state to the deviatoric stress at failure based on the Mohr-Coulomb failure criterion, and (2) Tensile Stress Level (TSL), defined as the ratio of pore pressure ( $P_p$ ) to the minimum principal stress ( $S_3$ ).

$$SSL = \frac{\sigma_1 - \sigma_3}{\sigma_1|_f - \sigma_3} \quad (1)$$

$$TSL = \frac{P_p}{S_3} \quad (2)$$

where  $\sigma_1$  and  $\sigma_3$  are the maximum and minimum effective stresses for each cell at each timestep. SSL and TSL range from 0 to 1, with higher values indicating a greater likelihood of shear and tensile failure, respectively. We apply the Mohr-Coulomb failure criterion to calculate the breakdown effective stress ( $\sigma_1|_f$ ) as follows:

$$\sigma_1|_f = 2C_0 \frac{\cos \phi}{1 - \sin \phi} + \sigma_3 \frac{1 + \sin \phi}{1 - \sin \phi} \quad (3)$$

where  $C_0$  and  $\phi$  represent cohesion and the friction angle, respectively. By varying cohesion, we assess the model's sensitivity to existing geological discontinuities.

### Results and Discussion

The initial stress maps, obtained from finite element gravitational and tectonic loading, show an increasing trend in both maximum and minimum principal stress magnitudes ( $S_1$  and  $S_3$ ) toward the northeast, influenced by the structural trend of increasing reservoir depth in that direction (Figure 2). The stress maps in Figure 2 also indicate that the vertical stress is the maximum principal stress ( $S_1 = S_v$ ), confirming a normal stress regime in the study area. In Figure 2, we highlight the dominant North-South orientation of the minimum horizontal stress ( $S_{hmin}$ ) using an azimuthal arrow. These observations are consistent with recent findings from the Norwegian North Sea, supported with several high-quality Extended Leak Off Test (XLOT) subsurface stress data (Andrews et al., 2016; Thompson et al., 2022).

The CO<sub>2</sub> saturation and pressure buildup maps in Figure 3 clearly reveal the significant influence of stress anisotropy, structural heterogeneity, and rock properties on the asymmetric CO<sub>2</sub> plume shape and pressure distribution after 20 years of injection into Well\_1. The dominant east-west

orientation of maximum horizontal stress in the model, combined with permeability anisotropy and gravitational forces toward the shallower western part of the reservoir, effectively explains the preferential migration of the CO<sub>2</sub> plume toward the west.

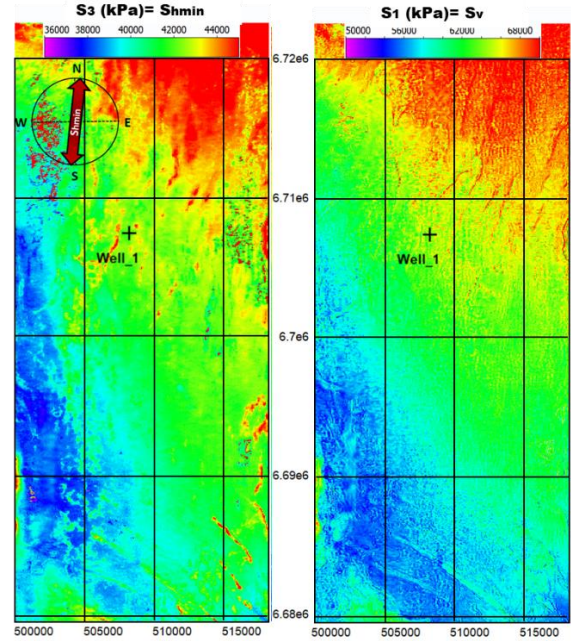


Figure 2: Reservoir initial stress maps before CO<sub>2</sub> injection.

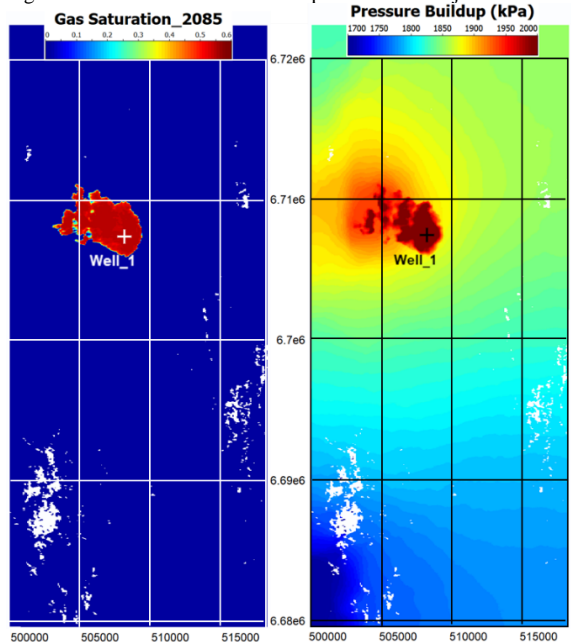


Figure 3: Reservoir pressure buildup and gas saturation maps at the end of the CO<sub>2</sub> injection period in 2085.

## Geomechanical risk assessment for CO<sub>2</sub> storage in the North Sea's Luna site

Additionally, Figure 3 highlights that the excessive pressure buildup (i.e., the difference between the current pressure and the initial pore pressure of the aquifer) near the wellbore gradually dissipates toward the edges of the model. This indicates the long-distance migration of the pressure plume from the injector, which could potentially activate critically stressed faults tens of kilometers away from the injector. Injection-induced effective stress decrease leads to heave within the reservoir, pushing the overburden layers upward. Depending on their poroelastic properties, this displacement can propagate to the surface, resulting in seabed uplift. Figure 4 shows approximately 1.3 cm of seabed uplift in response to a 2 MPa pressure buildup near the wellbore at the end of 20 years of CO<sub>2</sub> injection. This level of uplift is considered reasonable and safe for offshore surface facilities (Equinor, 2020).

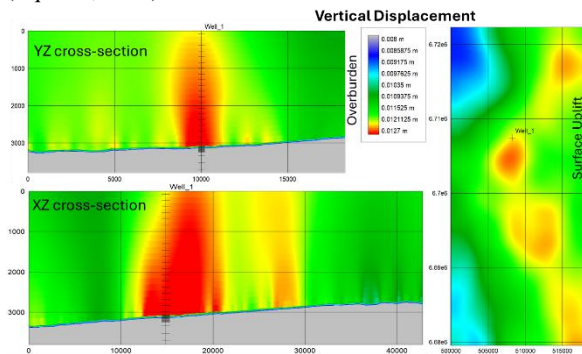


Figure 4: Vertical displacement cross sections and surface uplift map at the end of the CO<sub>2</sub> injection period in 2085.

Our main contributions are the SSL and TSL analyses derived from the calculated stress, pore pressure, and breakdown stress (based on the Mohr-Coulomb failure criterion) for each cell at each timestep (Figure 5). The SSL and TSL maps in Figure 5 provide a quantitative assessment of geomechanical risks associated with caprock integrity for the Luna aquifer in our study area. SSL and TSL values below 0.5 and 0.78, respectively, demonstrate the safety of the storage operation, indicating a low risk of caprock mechanical leakage for long-term CO<sub>2</sub> storage in the Luna aquifer.

Additionally, Figure 5 demonstrates the remarkable influence that small-scale heterogeneity and stress anisotropy exert on the spatial distribution of SSL and TSL, as well as the risk of caprock failure. These critical details are often overlooked in coarse-grid reservoir geomechanical models, potentially resulting in misleading assessments for many subsurface storage projects.

The findings also have broader implications for hydrogen storage and geothermal energy projects, demonstrating the potential of integrated geomechanical modeling approaches to inform the safe and efficient deployment of other subsurface injection technologies.

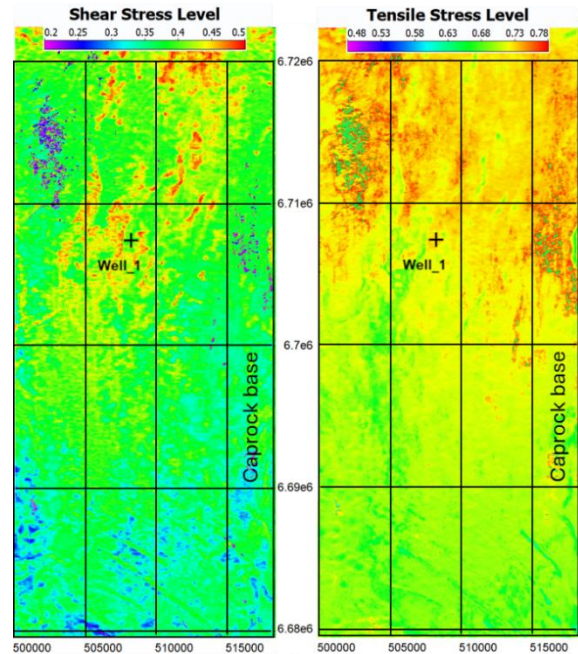


Figure 5: SSL and TSL maps at the base of caprock at the end of the CO<sub>2</sub> injection period in 2085.

## Conclusions

In conclusion, our high-fidelity geomechanical modeling of CO<sub>2</sub> injection into the Luna aquifer provides valuable insights into the complex interactions between stress anisotropy, structural heterogeneity, and pressure buildup in the Norwegian North Sea. The SSL and TSL analyses demonstrate the robustness of our approach in assessing geomechanical risks, showing that caprock integrity is maintained with low mechanical leakage risk throughout the 20-year injection period. The spatial distribution of SSL and TSL highlights the critical role of small-scale heterogeneity and stress anisotropy, underscoring the importance of high-resolution models for accurate risk assessment. Our findings not only enhance the understanding of CO<sub>2</sub> storage safety but also offer broader implications for other subsurface injection technologies, such as hydrogen storage and geothermal energy. This study reinforces the necessity of integrated geomechanical modeling in ensuring the safe and efficient deployment of carbon storage and other sustainable energy solutions.

## Acknowledgments

We thank the Viridien Earth Data (EDA) team for permission to publish results from this multi-client study.

## REFERENCES

- Andrews, J. S., et al., 2016, Use of unique database of good quality stress data to investigate theories of fracture initiation, fracture propagation and the stress state in the subsurface: Proceedings of the 50th U.S. Rock Mechanics/Geomechanics Symposium, 26–29 June, Houston, Texas, ARMA-2016-887.
- Bachu, S., 2013, Drainage and imbibition CO<sub>2</sub>/brine relative permeability curves at in situ conditions for sandstone formations in western Canada: *Energy Procedia*, **37**, 4428–4436.
- Bachu, S., and J. J. Adams, 2003, Sequestration of CO<sub>2</sub> in geologic media: Integration of science and engineering: *GSA Today*, **13**, 11, 4–10.
- Booth, M., R. Porjesz, G. Duval, S. Otto, P. Park, et al., 2021, Basin-scale CO<sub>2</sub> storage site screening – An example from the Northern North Sea Basin (UK/Norway): SPE Virtual Workshop: IRMS – Carbon Cycle Management.
- Bretan, P., G. Yielding, O. M. Mathiassen, and T. Thorsnes, 2011, Fault-seal analysis for CO<sub>2</sub> storage: An example from the Troll area, Norwegian Continental Shelf: *Petroleum Geoscience*, **17**, 2, 181–192.
- Burnside, N. M., and M. Naylor, 2014, Review and implications of relative permeability of CO<sub>2</sub>/brine systems and residual trapping of CO<sub>2</sub>: *International Journal of Greenhouse Gas Control*, **23**, 1–11.
- Equinor, 2020, 25 years of successful offshore CO<sub>2</sub> storage in Norway: Retrieved from <https://cdn.equinor.com/files/h61q9gi9/global/5972f8e7d34e8c548d284e6d51cc5cbeb7bf683d.pdf>.
- Harvey, A. H., 1996, Semiempirical correlation for Henry's constant over large temperature ranges: *AIChE Journal*, **42**, 1491–1494.
- Haghi, A. H., and R. Chalaturnyk, 2024, Relative permeability evolution with thermo-poromechanical process during N<sub>2</sub> and scCO<sub>2</sub> injection in brine saturated Deadwood sandstone from Aquistore: *International Journal of Greenhouse Gas Control*, **135**, 104159.
- Haghi, A. H., R. Chalaturnyk, and H. Ghobadi, 2018, The state of stress in SW Iran and implications for hydraulic fracturing of a naturally fractured carbonate reservoir: *International Journal of Rock Mechanics and Mining Sciences*, **105**, 28–43.
- Haghi, A. H., R. Chalaturnyk, M. J. Blunt, K. Hodder, and S. Geiger, 2021, Poromechanical controls on spontaneous imbibition in earth materials: *Scientific Reports*, **11**, 1, 1–11.
- Haghi, A. H., R. Kharrat, M. R. Asef, and H. Rezaadegan, 2013, Present-day stress of the central Persian Gulf: Implications for drilling and well performance: *Tectonophysics*, **608**, 1429–1441.
- Haghi, A., S. Otto, and G. Duval, 2024, Geomechanical assessment of potential CO<sub>2</sub> storage sites in the US shallow water Gulf Coast, SSRN Electronic Journal, 2014646, doi: <https://doi.org/10.2139/ssrn.5014649>.
- Haghi, A. H., S. Talman, and R. Chalaturnyk, 2020, Consecutive experimental determination of stress-dependent fluid flow properties of Berea sandstone and implications for two-phase flow modelling: *Water Resources Research*, **56**, 1, WR024245.
- Haghi, A. H., S. Talman, and R. Chalaturnyk, 2019, Stress-dependent pore deformation effects on multiphase flow properties of porous media, *Scientific Reports*, **9**, 1, 1–10.
- Han, Y., H. H. Liu, K. Alruwaili, and M. J. AlTammar, 2024, Wellbore and caprock integrity during CO<sub>2</sub> injection in saline aquifer: *International Petroleum Technology Conference*, D021S053R006.
- Li, Y., H. Yang, B. Li, and Z. Li, 2025, Interference behaviour between bedding planes and hydraulic fractures and its influence on the complex fracture network in shale: *Rock Mechanics and Rock Engineering*, **58**, 1, 181–201.
- Thompson, N., J. S. Andrews., L. Wu, and R. Meneguolo, 2022, Characterization of the in-situ stress on the Horda platform – A study from the Northern Lights Eos well: *International Journal of Greenhouse Gas Control*, **114**, 103580.
- Norwegian Petroleum Directorate, n.d., CO<sub>2</sub> Atlas for the Norwegian Continental Shelf – Geology of the North Sea: Retrieved from <https://www.sodir.no/en/whats-new/publications/CO2-atlases/CO2-atlas-for-the-norwegian-continental-shelf/4-the-norwegian-north-sea/4.1-geology-of-the-north-sea/>.
- Pruess, K., and J. García, 2002, Multiphase flow dynamics during CO<sub>2</sub> disposal into saline aquifers: *Environmental Geology*, **42**, 2–3, 282–295.
- Rutqvist, J., J. T. Birkholzer, and C. F. Tsang, 2008, Coupled reservoir–geomechanical analysis of CO<sub>2</sub> injection and ground deformations at In Salah, Algeria: *International Journal of Rock Mechanics and Mining Sciences*, **45**, 8, 1321–1335.
- Sengupta, M., J. Dai, S. Volterrani, N. Dutta, N. S. Rao, B. Al-Qadeeri, and V. K. Kidambi, 2011, Building a seismic-driven 3D geomechanical model in a deep carbonate reservoir: 81st Annual International Meeting, SEG.
- Sibson, R. H., 2017, Tensile overpressure compartments on low-angle thrust faults: *Earth, Planets and Space*, **69**, 1–15.
- Vilarrasa, V., and J. Carrera, 2015, Geomechanical impacts of geological carbon storage on deep saline aquifers: *International Journal of Greenhouse Gas Control*, **24**, 1–16.
- Wang, Y., Z. Zhang, C. Vuik, and H. Hajibeygi, 2024, Simulation of CO<sub>2</sub> storage using a parameterization method for essential trapping physics: FluidFlower benchmark study: *Transport in Porous Media*, **151**, 5, 1053–1070.
- Zeidouni, M., 2024, Transient pressure interference during CO<sub>2</sub> injection in saline aquifers: *SPE Journal*, 1–12.
- Zhao, R., J. Cheng, and K. Zhang, 2012, CO<sub>2</sub> plume evolution and pressure buildup of large-scale CO<sub>2</sub> injection into saline aquifers in Sanzhao depression, Songliao Basin, China: *Transport in Porous Media*, **95**, 407–424.
- Zoback, M. D., and S. M. Gorelick, 2012, Earthquake triggering and large-scale geologic storage of carbon dioxide: *Proceedings of the National Academy of Sciences*, **109**, no. 26, 10164–10168.